

Fig. 1 Geometry of the characteristics solution.

enough real characteristics for an MOC to be useful. Nemchinov⁴ recognized that the equations of unsteady radiative gasdynamics, at least to a differential approximation, possess hyperbolic character. The usefulness of his observation seems not to have been generally accepted, and its implications have not been exploited previously. Thus, in this investigation, a characteristic method is developed for general problems including upstream absorption. Application is then made to both planar and nonplanar situations, the former within the framework of both the differential approximation and the transfer equation. The formulation does not rely upon the assumptions of a gray gas or the existence of local thermodynamic equilibrium which are invoked.

II. Verification of Hyperbolicity

The equation of transfer in a gray gas in local thermodynamic equilibrium is^{5,6}

$$\beta(\partial I/\partial t) + \Omega \cdot \text{grad}(I) = \tau_l \alpha (B - I) \quad (2.1)$$

where the frequency integrated specific intensity I and the black body steradiancy B are normalized by the black body flux in the undisturbed medium, and the characteristic time is that for propagation of isothermal disturbances across the region of interest $l/(RT_\infty)^{1/2}$. The sound-light parameter and Bouguer number are, respectively,

$$\beta = (RT_\infty)^{1/2}/C, \quad \tau_l = \alpha_\infty l \quad (2.2)$$

If Eq. (2.1) is multiplied by the general tensor $\bar{\Omega}^n$, where Ω is the unit vector in the direction of propagation, and successively integrated over the unit sphere, the first few moment equations are

$$\beta(\partial I_0/\partial t) + \text{div} \mathbf{I}_1 = \tau_l \alpha (4\pi B - I_0) \quad (2.3)$$

$$\beta(\partial \mathbf{I}_1/\partial t) + \text{div} \bar{\mathbf{I}}_2 = -\tau_l \alpha \mathbf{I}_1 \quad (2.4)$$

where

$$\bar{\mathbf{I}}_n = \int_{4\pi} \bar{\Omega}^n I(\Omega, \mathbf{r}, t) d\Omega \quad (2.5)$$

The moment \mathbf{I}_1 is the heat flux, and $\bar{\mathbf{I}}_2$ is the radiative stress tensor. Although β is generally small, it is retained for completeness. There are situations of considerable interest (early stages of blasts⁷) in which $t \sim 10^6$ K, hence $\beta \sim 10^{-3}$, $\beta/B_0 \sim 0(1)$, so that both parameters cannot necessarily be ignored. Whether one assumes \mathbf{I}_1 to be specified by the intensity so that Eq. (2.1) determines the radiative field or I is to be specified by its moments so that the sequence of which Eqs. (2.3) and (2.4) are the first members is required, the system of equations appears to be hyperbolic.

Since the gasdynamics appear at most through in homogeneous terms in the equations which govern the radiative variables, the characteristic surfaces due to radiation may be investigated immediately. Although the system is not closed, if all moments are retained it may be deduced that⁸ if $\psi(\mathbf{r}, t) = \text{const}$ is a characteristic manifold, then,

$$\lim_{M \rightarrow \infty} (\beta \psi_t)^M = 0 \quad (2.6)$$

where subscript notation is employed for partial differentiation. These are cylindrical manifolds $\psi = \psi(\mathbf{r})$ with generatrices parallel to the time axis. The confluence of these manifolds is the photon path line $d\mathbf{r} = \Omega dt/\beta$ since the infinite sequence of moments specifies the intensity uniquely. If a spherical harmonic expansion² is applied, the sequence Eqs. (2.3) and (2.4) . . . is formally equivalent to Eq. (2.1). If the expansion is truncated at the spherical harmonic $Y_N^m(\Omega)$, the elements of the N th row of the radiative characteristic determinant are moved from the right to the left of the major diagonal so that $(N-1)/2$ characteristic hypercones appear if N is odd and $(N-2)/2$ if N is even. For instance, to a P_1

approximation

$$\bar{\mathbf{I}}_2 = (I_0/3)\bar{\mathbf{I}} \quad (2.7)$$

so that Eqs. (2.3) and (2.4) lead to

$$3\beta^2(\psi_t)^2 = (\text{grad } \psi)^2 \quad (2.8)$$

which are light cones, $(t - t_0)^2 = 3\beta^2(\mathbf{r} - \mathbf{r}_0) \cdot (\mathbf{r} - \mathbf{r}_0)$. Since the time axis lies within the cone, the radiative disturbance must eventually be spread over all of space. As $\beta \rightarrow 0$, Eq. (2.8) no longer defines a time-like direction but does lead to the real characteristic surface, $t = \text{const}$. By the usual definition⁹ the problem is still hyperbolic. Actually, until the expansion is terminated the system is parabolic since only one compatibility relation, Eq. (2.1) exists. The gasdynamic variables possess the usual particle paths and Mach conoids with modified Mach angles to be discussed shortly.

The hyperbolicity of the unsteady equations of radiative gasdynamics is best illustrated if attention is restricted to one spatial dimension and time. The equations of ideal radiative gasdynamics to $O(\beta^2)$ are, in the approximation noted previously⁶:

$$(\partial \mathbf{V}/\partial r) + \bar{\mathbf{M}} \cdot (\partial \mathbf{V}/\partial t) = \mathbf{N}(\mathbf{V}, r, t) \quad (2.9)$$

$$\mathbf{V} = \{P, u, T, I_0, q\} \quad (2.10)$$

$$\bar{\mathbf{M}} = \begin{bmatrix} -\frac{A_2}{u\Delta} & \frac{C_P \rho}{T \Gamma u^2 \Delta} & 0 & 0 & 0 \\ \frac{T A_2}{P u^2 \Delta} & -\frac{A_2}{u\Delta} & 0 & 0 & 0 \\ -\frac{T^2 A_1}{u^2 \Delta} & \frac{T A_1}{u^2 \Delta} & \frac{1}{u} & 0 & 0 \\ 0 & 0 & 0 & 0 & 3\beta \\ 0 & 0 & 0 & \beta & 0 \end{bmatrix} \quad (2.11)$$

$$\mathbf{N} = \begin{bmatrix} \frac{1}{\Delta} \left\{ \frac{j P C_P}{\Gamma r} - \frac{\tau_l Q}{u B_0} + \frac{\beta \tau_l \alpha}{B_0} q \left[\frac{C_P T}{\Gamma u^2} + 3 \right] \right\} \\ \frac{1}{\rho u^2 \Delta} \left\{ -j \frac{P u C_P}{\Gamma r} + \frac{\tau_l Q}{B_0} + \frac{\beta \tau_l \alpha}{B_0} \times \right. \\ \left. q \left[A_1 - 3 - \frac{C_P}{\Gamma} \right] \right\} \\ \frac{1}{\rho u \Delta} \left\{ j \frac{A_1 P u}{r} - \frac{\tau_l Q}{B_0} \left[1 - \frac{T}{u^2} \right] + \right. \\ \left. \frac{\beta \tau_l \alpha}{B_0} q \left[\frac{A_1 T}{u^2} + 3 \left(1 - \frac{T}{u^2} \right) \right] \right\} \\ -3\tau_l \alpha q \\ -(\tau_l Q + j q/r) \end{bmatrix} \quad (2.12)$$

where

$$C_P = 1 + 4\Gamma \beta I_0 / 3 P B_0 \quad (2.13)$$

$$A_1 = 1 + 4\beta I_0 / 3 P B_0 \quad (2.14)$$

$$A_2 = A_1 + C_P / \Gamma \quad (2.15)$$

$$\Delta = A_1 - C_P (1 - T/u^2) / \Gamma \quad (2.16)$$

All properties are normalized by their values in the undisturbed gas. Enthalpy and density have been removed through the thermodynamic ($h = T$) and state ($P = \rho T$) relations. In addition

$$\begin{aligned} Q &= \alpha(I_0 - 4\pi B) \\ B_0 &= \rho_\infty (RT_\infty)^{3/2} / \sigma T_\infty^4 \\ \Gamma &= (\gamma - 1) / \gamma \end{aligned} \quad (2.17)$$

The characteristic directions of the quasi-linear system Eq. (2.9) are the eigen values of \mathbf{M} . Similarly the left-hand eigen vectors of \mathbf{M} determine the compatibility relations when dotted into Eq. (2.9). If there are as many distinct eigen vectors as there are elements in \mathbf{V} , the system is hyperbolic (if some of the eigen values are degenerate the system is symmetric hyperbolic), and a numerical method of characteristics may be applied. If there are less eigen vectors than elements in \mathbf{V} , the system is parabolic. As $\beta \rightarrow 0$ Eqs. (2.3) and (2.4) apply along $t = \text{const}$; therefore, even with radiation, the system is symmetric hyperbolic. It may be shown that in the Rosseland limit ($\tau_l \gg 1$) $4\pi B \simeq I_0$, and the system of equations reverts from hyperbolic to parabolic character. Hence the singular nature of this approximation. Retention of I_0 bridges the gap between q and T and always leads to hyperbolicity.

Once the hyperbolic nature of the equations is recognized, the following compatibility relations may be written:

$$d\pm P/dt \pm \rho ad\pm u/dt = \tau_l \Gamma Q/B_0 C_P (1 - \Gamma) - jPu/r(1 - \Gamma) \quad (2.18)$$

on the lines $dr/dt = u \pm a$, where

$$a^2 = T(1 + 4\Gamma\beta I_0/3PB_0)/(1 - \Gamma) \quad (2.19)$$

Also

$$dT/dt - (\Gamma A_1 T/PC_P)dP/dt = \tau_l QT/B_0 PC_P \quad (2.20)$$

on the path line $dr/dt = u$, and

$$(3)^{-1/2} d\pm/dr [I_0 \pm q(3)^{1/2}] = \pm \tau_l \alpha [4\pi B \mp q(3)^{1/2} - I_0] \mp jq/r \quad (2.21)$$

on the light lines, $dr/dt = \pm 1/\beta(3)^{1/2}$. In all of the preceding, $j = 0, 1$, or 2 for planar, cylindrical, or spherical geometries respectively. The modifications of the specific heat and acoustic speed are due to radiation pressure and energy density, which appear isotropically to this approximation. As $\beta \rightarrow 0$ the radiative characteristic directions coincide, but Eq. (2.21) remain distinct and the system is hyperbolic. The generalization of these relations to nongrey gases with chemical nonequilibrium may be found in Ref. 8.

III. Consequences of Hyperbolicity and Truncation of the Spherical Harmonic Expansion

It is known that hyperbolic systems of equations admit generalized or weak solutions with discontinuities in the dependent variables (shock waves) so that the governing equations cannot be satisfied locally.¹¹ If the governing equations are written in divergence form and the types of discontinuities allowed are examined, the manifolds across which these discontinuities occur may be determined. If the procedure is applied to Eq. (2.9), it follows that

$$\rho_1(u_1 - u_s) = \rho_2(u_2 - u_s) \quad (3.1)$$

$$P_1 + (\beta I_0/3B_0)_1 + \rho_1 u_1(u_1 - u_s) = P_2 + (\beta I_0/3B_0)_2 + \rho_2 u_2(u_2 - u_s) \quad (3.2)$$

$$\Gamma q_1/B_0 + \rho_1 H_1(u_1 - u_s) + (\Gamma\beta/B_0)I_{01}(4u_1/3 - u_s) = \Gamma q_2/B_0 + \rho_2 H_2(u_2 - u_s) + (\Gamma\beta/B_0)I_{02}(4u_2/3 - u_s) \quad (3.3)$$

$$\begin{bmatrix} \beta u_s & -1 \\ -1 & 3\beta u_s \end{bmatrix} \begin{Bmatrix} I_{01} \\ q_1 \end{Bmatrix} = \begin{bmatrix} \beta u_s & -1 \\ -1 & 3\beta u_s \end{bmatrix} \begin{Bmatrix} I_{02} \\ q_2 \end{Bmatrix} \quad (3.4)$$

where the discontinuities occur across the line $dr/dt = u_s$ and the stagnation enthalpy is $H = T + \Gamma u^2/2$. Equation (3.1-3.3) are identically the relations derived differently by Sachs¹⁰ and Marshak.¹² I_0 and q must be continuous across all shocks except those for which $u_s = 1/\beta(3)^{1/2}$. As more moments are retained this slope approaches the speed of

light. If $0(\beta/B_0)$ were neglected, the ordinary Rankine-Hugoniot relations would follow.

It has been observed^{8,13} that as $\beta \rightarrow 0$ the radiation moment equations become stiff.¹⁴ This is illustrated by the planar situation wherein the existence of only one important direction cosine allows all moments of the specific intensity to be represented by scalars. The sequence generated by Eqs. (2.3) and (2.4) as $\beta \rightarrow 0$ may be written in the form

$$\partial I_1/\partial I_2 = (I_0 - 4\pi B)/I_1 \quad (3.5a)$$

$$\partial I_2/\partial I_3 = I_1/(I_2 - 4\pi B/3) \quad (3.5b)$$

Since $I \rightarrow B$ as radiative equilibrium is attained, an equilibrium state is singular. Since the spatial derivatives of the dependent variables vanish while the phase derivatives Eq. (3.5) are indeterminate, it can be shown that a saddle occurs. If all moments of the intensity are retained, the equilibrium state is a regular point of the transfer equations; however, truncation of the moments forces a saddle always to occur. This saddle is similar to that which has been observed in the upstream state of radiatively structure shock waves.¹⁵ The appearance of an upstream saddle is a consequence of both the omission of terms of order β and truncation of the system of moment equations. It is solely peculiar to neither this problem nor that of Ref. 15. If either restriction is relaxed an upstream saddle should not appear for the gas models considered.

The hyperbolic character of the equations of unsteady radiative gasdynamics allows one to determine quite easily what data are necessary in order to specify a problem. If $0(\beta)$ is neglected, initial data on I_0 and q are not acceptable. The question of boundary data appropriate for the various orders of differential approximation has not been resolved. Most investigators prefer the Marshak condition of neutron transport theory¹⁶ with a P_1 differential approximation.

A method of images has been devised¹⁷ whereby boundary data consistent with a P_1 approximation may be derived. Because of the angular averaging performed upon the radiative field, specularly reflecting surfaces are not generally allowed. At a boundary whose outward normal is in the direction of increasing r ,

$$I_{0W} + (2 - \epsilon)q_W(3)^{1/2}/\epsilon = 4\pi B(T_W) \quad (3.6)$$

$$I_{0W} = 2\pi\epsilon B(T_W) + \left(1 - \frac{\epsilon}{2}\right) \times (3)^{1/2} \int_0^\infty F_j(\eta') \exp[-(3)^{1/2}\tau_l\eta'] d\eta' \quad (3.7)$$

where

$$\eta = \int_{R_p(t)}^r \alpha(\xi, t) d\xi \quad (3.8a)$$

$$F_j = 4\pi\tau_l B - jq/\alpha r \quad (3.8b)$$

and ϵ is the emissivity of the surface which is located at $R_p(t)$ and whose temperature is $T_W(t)$. Equation (3.6) is the generalization of Mark's boundary condition.¹⁶

IV. Application of the Theory of Characteristics to One-Dimensional Piston Problems

The theory of characteristics has been applied to the determination of flowfields generated by one-dimensional pistons inserted into initially undisturbed gases. Only the limit $\beta \rightarrow 0$ is considered. Since the entire flowfield must be known at each time chosen, only the constant time approach¹⁸ is appropriate. The iteration scheme for which Courant, Isaacson, and Rees¹⁹ have proved convergence will be assumed. Since all of the past and the present will affect every point, the domain of dependence is not violated by the difference equations although the Courant, Friedrichs, Lewy stability criterion is satisfied.

Inclusion of Upstream Absorption and Passage through the Saddle Point

It is assumed that I_0 is known on the piston path, so that Eq. (2.21) applies along a constant time line from below each point. At a field point, simultaneous solution of the difference forms of Eqs. (2.18), (2.20), and (2.21) yields all properties at point 1 (Fig. 1a) in addition to the locations of points 2-4, point 5 having been specified a priori. Similarly at a point on the boundary (Fig. 1b) the velocity is known so that Eq. (2.18) and $dr/dt = u - a$ along the left running characteristic yield the location of point 3 and the pressure at point 1. Eq. (2.20) on the piston specifies the temperature.

If the shock is extrapolated from its last location with the most recent slope, points (1, 7) of Fig. 1c are determined successively in the standard manner. Although there are fifteen quantities to be determined, the four radiative variables are determined trivially by Eqs. (2.21) and (3.4). In accordance with the iterative scheme P , u , and T are determined to a first approximation at point 1 by the properties at points 2-4 upstream of the shock. Equation (3.2) and the difference form of Eq. (2.18) along the right running characteristic may be combined to yield

$$P_6 + R_{6,7}^{(M)} \Delta t - [P_1 + \rho_1 u_1^2] + (\rho a)_{6,7} u_6 + u_7 [\rho_1 u_1 - (\rho a)_{6,7}] + \rho_1 u_6 (u_1 - y_7) = 0 \quad (4.1)$$

where $R^{(M)} = \Gamma(\tau_1 Q/B_0 - jPu/\Gamma r)/(1 - \Gamma)$. The double subscript denotes an average value between two points, and Δt is the time increment of the difference scheme. This may be solved iteratively with the remaining Rankine-Hugoniot equations in order to determine the shock velocity. The procedure is that which must be employed in order to determine flowfields behind shock waves moving into any nonuniform gas. Once the shock is traversed, the entire upstream flowfield may be determined.

Even if I_0 were known at the piston surface, the governing equations could not be integrated numerically through the saddle point. It is of interest to inquire into the criteria which allow one to claim to have reached the saddle. Suppose I_0 were known at the wall sufficiently accurately that at some point $r_0(t)$ upstream of the shock radiative equilibrium were nearly attained. Consistent perturbation about the saddle leads one to conclude that if

$$I_0 = 4 + \epsilon_1 I'_0 + 0(\epsilon_1^2), \quad q = \epsilon_1 q' + 0(\epsilon_1^2) \quad (4.2)$$

where $\epsilon_1 \ll 1$ is characteristic of the deviation from equilibrium, it follows that

$$I'_{0rr} + jI'_{0r}/r - 3\tau_1^2 I'_0 = 0 \quad (4.3)$$

The equation admits exponentially divergent solutions. (This is a consequence of the more general proof of the existence of a saddle.) Since integration was initiated at the boundary, both q and I_0 are known at r_0 , thus, divergence must ensue unless

$$\chi = \{I_0(r_0) - 4\} F_j(r_0) - (3)^{1/2} q(r_0) \sim 0(\epsilon_1^2) \quad (4.4a)$$

where

$$F_j(r_0) = \begin{cases} 1 & j = 0 \\ K_1[\tau_1 r_0(3)^{1/2}]/K_0[\tau_1 r_0(3)^{1/2}] & j = 1 \\ 1 + 1/r_0 \tau_1(3)^{1/2} & j = 2 \end{cases} \quad (4.4b)$$

and the K_n are modified Bessel functions. For large $r_0 \tau_1$ all of the F_j are the same, and Eq. (4.4a) is an alternative statement of the Mark condition for the incoming intensity. It follows as well that for $r > r_0$,

$$\begin{aligned} q(r)/q(r_0) &\simeq u(r)/u(r_0) \simeq [P(r) - 1]/[P(r_0) - 1] \simeq \\ &[T(r) - 1]/[T(r_0) - 1] \simeq \\ &[I_0(r) - 4]/[I_0(r_0) - 4] \simeq G_j(r, r_0) \end{aligned} \quad (4.5a)$$

where

$$G_j(r, r_0) = \begin{cases} \exp[-(r - r_0)\tau_1(3)^{1/2}] & j = 0 \\ K_0[r\tau_1(3)^{1/2}]/K_0[r_0\tau_1(3)^{1/2}] & j = 1 \\ (r/r_0) \exp[-(r - r_0)\tau_1(3)^{1/2}] & j = 2 \end{cases} \quad (4.5b)$$

The P_1 moment equations have infinitely many integral curves. Only the one which satisfies an upstream Mark condition, Eq. (4.4a), will pass smoothly toward radiative equilibrium. If upstream absorption and emission are ignored, then $I_0 - q(3)^{1/2} = 0$ at the shock. If the freestream is allowed to emit, $I_0 - q(3)^{1/2} = 4$ thereat. If upstream absorption and/or emission are neglected the gas immediately downstream of the shock is not in radiative equilibrium, there is no saddle, and the solution curve is no longer specified by its behavior near equilibrium. Therefore a solution which satisfies a Marshak condition is acceptable. In any bounded region a Marshak condition provides favorable cancellation of errors inherent in the P_1 approximation (as is shown in Ref. 20). In an unbounded medium it leads to divergence from radiative equilibrium. The divergence may not be serious, but in practice the degree of divergence is uncertain, and linearization about the singular point indicates that only a Mark condition should be used.

Over-all Numerical Procedure

Examination of the compatibility relations, Eqs. (2.18), (2.20), and (2.21) leads one to consider two possible iterative approaches. In both schemes, the properties P_1 , U_1 , and T_1 may be found independent of I_0 , and q_1 to lowest order because the averaged coefficients and inhomogeneous terms always lag the dependent variables by a full iteration. The first scheme (Method I) involves guessing a value of I_0 at the wall and integrating upward and forward simultaneously, carrying out iteration for all properties at each point individually. Passage through the saddle would not be assured unless I_0 were guessed correctly at the wall; therefore, once divergence were detected the calculation could be reinitiated with a new guess. The independence noted leads to another scheme (Method II). Since the gasdynamic variables can be found at as many points as desired to a first approximation by forward integration, Eq. (2.21) may be reduced to a quadrature, and I_0 and q may be found at all points consistent with P , U , and T . The iteration of the compatibility relations would then be carried out at all points simultaneously. Method II allows the exact solution to be obtained in the planar case. The common expressions then apply;²¹

$$\begin{aligned} Q(r, t) &= 2\pi\alpha \left\{ \epsilon B(T_w) E_2(\tau_1 \eta) + \right. \\ &\quad (1 - \epsilon) \int_{R_p}^{\infty} \tau_1 \alpha B(r') E_1[\tau_1(\eta + \eta')] dr' + \\ &\quad \left. \int_{R_p}^{\infty} \tau_1 \alpha B(r') E_1[\tau_1|\eta - \eta'|] dr' \right\} - 4\pi\alpha B \end{aligned} \quad (4.6)$$

$$\begin{aligned} q(r, t) &= 2\pi \left\{ \epsilon B(T_w) E_3(\tau_1 \eta) + \right. \\ &\quad (1 - \epsilon) \int_{R_p}^{\infty} \tau_1 \alpha B(r') E_2[\tau_1(\eta + \eta')] dr' + \\ &\quad \left. \int_{R_p}^{\infty} \tau_1 \alpha B(r') \operatorname{sgn}(r - r') E_2[\tau_1|\eta - \eta'|] dr' \right\} \end{aligned} \quad (4.7)$$

where

$$E_n(x) = \int_0^1 t^{n-1} \exp\left(-\frac{x}{t}\right) dt$$

are the Exponential Integrals.²² When Method II is applied, one is attempting the solution of the integro-differential equations by successive approximations. Although convergence is by no means assured, no difficulties were encountered in practice. Method II incorporates appropriate boundary data

and therefore requires no special saddle point approach. The difficulties arise again as convergence problems.

In Method I, a value of I_0 is required at the piston. Equation (3.7) provides a means of obtaining fairly accurate initial guesses based on the most recent flowfield. A method similar to that of Xerikos and Anderson²³ for passage through the sonic singularity of the integral approach to blunt body flows was chosen. Equations (4.4) provide a single quantity χ (I_{0w}) which allows prediction of corrected guesses. If there are no external sources of radiation, absorption is more important than emission until equilibrium is attained upstream, and the volumetric energy loss must change sign near the upstream side of the shock. Furthermore, the heat flux must tend monotonically to zero as integration proceeds toward the upstream gas. Thus, the point r_0 is taken at that station at which either $\text{div}(q)$ or q first changes sign from that which it had just upstream of the shock wave. Since χ must vanish for sufficiently large r_0 , a new value of I_0 may be found with linear influence coefficients. As the value of I_0 is improved, r_0 moves farther into the upstream gas. It is noted that if I_0 is too large at the wall, χ will be greater than zero when divergence occurs, and conversely. The method is like the moveable outer boundary technique of Scala and Gordon,²⁴ and it corresponds to the artifice of an optically black surface which radiates toward the shock layer but always remains far enough ahead of it so that negligible gasdynamic disturbance is generated.

Two procedures were employed for initiating the calculation, and both relied upon the assumption of frozen flow at the start of motion. First, if the wall is not too hot the shock wave is required to produce the elevated temperatures necessary for radiation. Since chemical excitation should precede radiation in all cases, nonradiating gasdynamics should be applied initially. It follows that the radiative field must be uncoupled from the gasdynamics, and a Maclaurin series in time may be carried out if the piston velocity is not large, the wall temperature is near unity, and $B_0 \gtrsim 0(1)$. To lowest order P , u , and T are functions of the conical variable $\xi \equiv r/t$, and may be found quite easily.²⁵ The corresponding radiative properties are, to order t^{j+2} ,

$$q = \left(\frac{t}{\xi}\right)^j \left\{ \int_{u_p}^{\tau} \xi^j f(\xi) d\xi + \epsilon \left[\left(\frac{16}{3^{1/2}}\right) \frac{dt}{dT_w} - \int_{u_p}^{u_s} \frac{\xi^j f(\xi) d\xi}{u_s^j} \right] / \left[\frac{\epsilon}{u_s^j} + \frac{(2-\epsilon)}{u_p^j} \right] \right\} \quad (4.8)$$

where $f(\xi) = 4\tau_l \alpha(\xi) [T^4(\xi) - 1]$. Also

$$I_0 \simeq 4 + 3^{1/2} q(\xi = u_s) + 0(t^8) \quad (4.9)$$

Since the volume of radiating gas vanishes as $t \rightarrow 0$, there can be no heat flux initially. The radiative properties thus predicted were generally reasonable, but if the shock were sufficiently strong and the initiating solution were applied for too large a value of t they were incorrect. As an alternative procedure, in many cases the radiation was turned on impulsively at some finite time by assuming that $\alpha = 0$ everywhere in the starting flowfield. This might be the case in a shock tube if the flow were initiated with a weakly absorbing gas and then large amounts of a strong absorber were injected. It may be demonstrated⁸ both analytically and numerically that as long as the correct nonradiating solution is applied for $0(\beta) \ll t \ll 1$ the subsequent motion must be correct and that the effect of the starting solution will be erased in a time comparable with the initiating instant.

Once solutions have been carried out it is of interest to interpret them in terms of an appropriate piston analogy.^{26,8} If transverse motion corresponds to piston insertion, steady-unsteady correspondence is achieved if

$$(B_0)_s K_H \gamma^{1/2} = (B_0)_u, [K_H = M_\infty \delta] \quad (4.10a)$$

$$(\alpha_\infty l)_s \delta = [\alpha_\infty (RT_\infty)^{1/2}]_u t_c^* \equiv (\tau_l)_u \quad (4.10b)$$

where l , the length of a finite body, corresponds to the characteristic time t_c^* at which piston motion is terminated. The subscripts s and u denote the corresponding steady and unsteady quantities, and δ is the (small) fineness ratio of the slender body. K_H , the hypersonic similarity parameter, is of order unity. If a slender wedge or cone (without characteristic physical length scale) is chosen, Eq. (4.10b) is unnecessary. Even though the axial direction is in general not time-like when radiative transfer is included, the usual hypersonic small disturbance approximations lead to the conclusion that axial convection predominates over axial transfer. In this case upstream influence is small (transverse influence outside of the shock layer is not, however) and a piston analogy holds.^{8,27,28} Since axial convection does not necessarily predominate near the nose, the piston analogy may be applied only to bodies whose slopes are continuous and only at distances from the nose such that $\alpha_R X \gg 16\Gamma\delta/3K_H(B_0)_s$. In addition, if the axial heat flux of the steady flow is expressed as $q^{(1)}/\sigma T_\infty^4 = \delta\gamma^4 K_H^8 \bar{q}^{(1)}$, the axial radiative field is determined by $\bar{q}^{(1)} = -(\partial I_0/\partial t)/3\alpha\tau_{lu}$.

V. Numerical Results and Discussion

To demonstrate the method, the insertion of planar and cylindrical pistons into ideal gases whose absorption properties were allowed to vary with temperature and pressure was investigated. The emissivities and temperatures of the piston surfaces could be specified arbitrarily, but in all cases discussed the wall was maintained at the temperature of the undisturbed gas. Unless otherwise noted, the low-temperature approximation to the Planck mean emission coefficient²⁹ was employed in all cases ($\alpha_P = PT^4$). The cases chosen for preliminary investigation employ combinations of parameters which preclude perturbation approaches, and heretofore unobserved phenomena will be reported. Long after the initiation of motion, the shock wave will precede the piston by such a large distance that it will be unaware of its existence. Although the agency which does work on the piston sustains the shock wave, the only effect of the surface will be to maintain the downstream velocity and temperature levels. Since radiative equilibrium will exist far up and downstream of the shock, at large times analyses such as that of Heaslet and Baldwin¹⁵ should be adequate for uniform piston motions; thus, attention is restricted to $t \lesssim 0(1)$.

Planar Flowfields

Exhaustive investigation confirmed that the frozen assumption is adequate in planar piston generated flows; thus, all results have been extrapolated to a vanishingly small initiating time in a manner similar to the h^2 procedure of Ref. 18. Through the divergence of the heat flux Eq. (2.17) only the first moment of the specific intensity I_0 appears in the energy equation. Thus, I_0 is the macroscopic property of the radiative field which exerts most influence on fluid mechanics. Since the differential approximation is worst in nearly optically thin flowfields, ($\tau_l \lesssim 1$), comparison of the exact and approximate results in such cases with moderate radiation is presented in Fig. 2. Exact solutions require Method II. Since Method I was much more rapid than Method II when the differential approximation was applied, it was employed in all final results. In general I_0 is underpredicted by the differential approximation when upstream absorption is neglected and overpredicted when it is retained. This is to be expected since the exact Exponential Integrals decay as $(1/x) \exp(-x)$ whereas the differential approximation lacks the algebraic factor. These predictions are in agreement with Kourganoff's astrophysical results.^{20,30} Both I_0 and q are accurate at the piston surface, usually within 5% of the exact values, but accuracy is better when upstream absorption is included. This accuracy can be attributed both to the consistent boundary condition Eq. (3.6) and to lack of appreciable

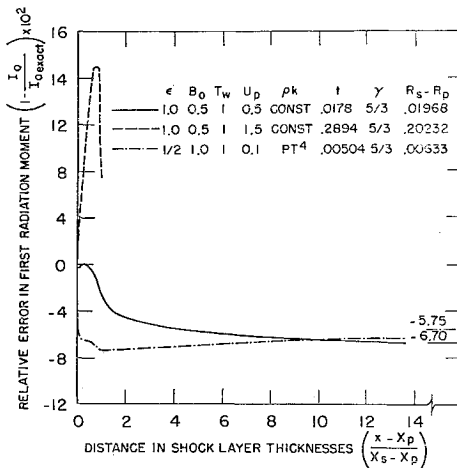


Fig. 2 A comparison of first radiative moment as predicted by the differential approximation and the full transfer equation.

anisotropy as indicated by $|q|/I_0 \lesssim 0.25$ (see Ref. 31 for the delineation of the anisotropy index). The cumulative effect of the differential approximation upon a flowfield which includes upstream absorption is indicated in Fig. 3. Although the error grows from piston to shock, surface properties are quite good. Since radiative effects upon both aerodynamics and heat transfer predicted by the differential approximation are sufficient for engineering purposes, all subsequent results employ the P_1 approximation.

Linearized analyses have predominated the literature in the past.²¹ If the piston velocity is small relative to the isothermal propagation speed and is constant, it may be shown that for $t \ll 1$ the velocity perturbation is

$$\frac{u}{u_p} = \lambda \exp(-\lambda x \gamma^{-1/2}) \int_0^{t-x\gamma^{-1/2}} \exp(\lambda \tau') \times \{I_{(0)}(\tau'') - 2\tau' I_{(1)}(\tau'')\} d\tau' + \gamma^{-1/2} \exp(-\lambda t) I_{(0)} \left[\lambda \left(t^2 - \frac{x^2}{\gamma} \right) \right] \quad (5.1)$$

$$\tau'' \equiv \lambda [\tau'(\tau' + 2x\gamma^{-1/2})]^{1/2}$$

where $\lambda = 8\tau_i \Gamma^2 / B_0$ and $I_{(0)}$ and $I_{(1)}$ are modified Bessel functions. Velocity perturbations downstream of the wavehead (at such small times upstream absorption is unimportant) as predicted by the MOC are compared for small times with linearized results of Eq. (5.1) in Fig. 4. The apparent discrepancy may be due to the greater importance of nonlinear interactions in radiative gasdynamics than in other nonequilibrium gasdynamic situations or to the application of the small time expansion beyond its region of validity. Since

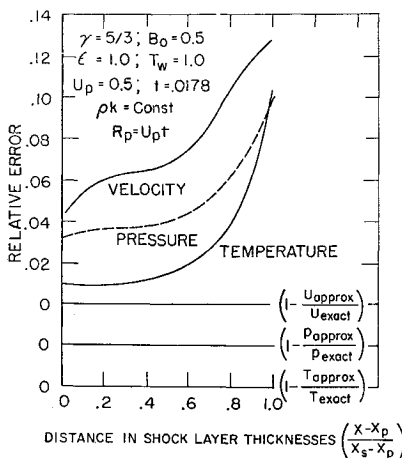


Fig. 3 Cumulative error in flowfields predicted by the differential approximation.

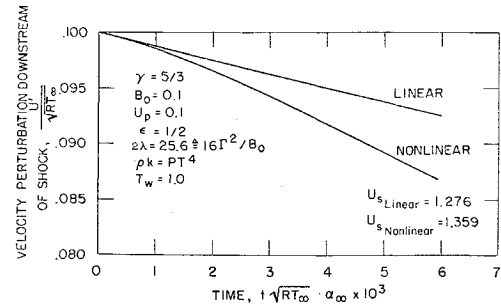


Fig. 4 Comparison of linear and nonlinear velocity perturbations downstream of wavehead.

the transforms of the linearized solutions for uniform piston motions cannot be easily inverted, more definite conclusions cannot be made. It is interesting that the discrepancy noted is of the order of the next correction to the linear theory.

Whereas linearized analyses tax one's manipulative skill for general piston paths, there is no difficulty in their investigation with the MOC. A uniformly decelerating piston whose path is given by $R_p = t(2 - t)$ may be interpreted as a two-dimensional ogive or as the lower surface of a slender biconvex airfoil whose angle of attack is four times its thickness ratio. The evolution of the pressure and temperature fields induced by such a piston is given in Figs. 5-7. The behavior of the velocity and pressure fields within the shock layer is qualitatively the same. The radiation-convection parameter $\tau_i / B_0 \sim 0(1)$ is realistic.[†] When radiation is moderate, a region in which large changes in entropy occur over small distances (an entropy layer) is apparent near the shock wave, whereas when radiation is weak ($\tau_i / B_0 \ll 1$) it may be demonstrated that the field is qualitatively that of a nonradiating gas. It is noted that a thin layer near the shock wave is more evident in pressure than in temperature. In blunt body flows, the pressure is insensitive to the radiative interaction; this seems not necessarily to be the case in slender body flows. One sees in Fig. 6 that the temperature of the gas at the wall approaches the wall temperature asymptotically for large times. Because the freestream resists shock layer energy losses through absorption and emission, the temperature decays more rapidly at the relatively unresisting black wall than at the shock wave. The importance of upstream absorption is illustrated by the behavior of the upstream temperature field, Fig. 7. Since upstream velocity disturbances are small, con-

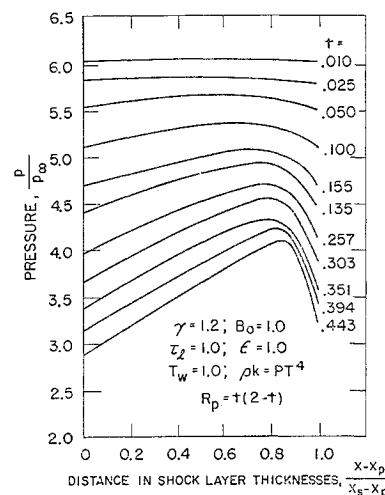


Fig. 5 Pressure field generated by a decelerating planar piston.

[†] The computations of Main and Bauer³² in hydrocarbon-air mixtures indicate that Planck and Rosseland mean absorption coefficients may be five orders of magnitude larger in a mixture which is half methylene (CH_2) and half air by volume than in air alone.

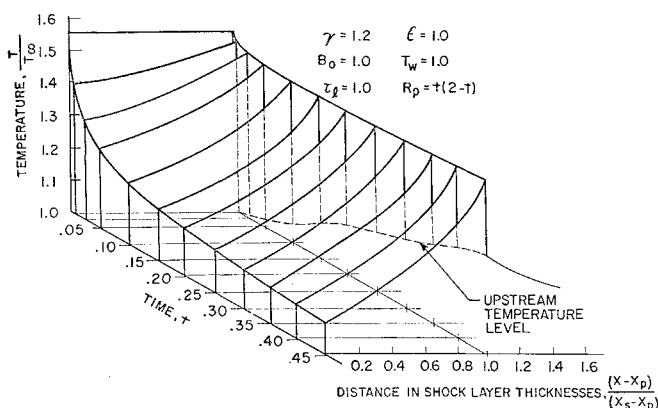


Fig. 6 Temperature field generated by a decelerating planar piston.

servation of mass requires that pressure and temperature fields must be at least qualitatively similar. Numerics⁸ verify this observation. Even at moderate times, temperature levels upstream may exceed those at points within the shock layer. Initially the shock layer is optically thin and energy is lost very rapidly to the upstream gas. As the piston decelerates, the shock engulfs preheated gas and recovers some of the energy which was lost in order to sustain itself. This is demonstrated by the appearance of a maximum in temperature immediately upstream of the shock wave. As dimensional considerations alone would dictate, the extent of upstream absorption is the order of the freestream absorption length, $1/\alpha_{\infty}$, which corresponds to fewer shock layer thicknesses the thicker the shock layer becomes. The evolution of the radiative field is typified by Fig. 8 in which the heat flux profiles are presented. For small times the linear variation characteristic of optically thin, nearly isothermal shock layers is apparent, and as the shock layer grows the heat flux becomes nearly constant with a severe optically thin region near the shock and a moderate one near the piston. More data than presented here reveals that whereas all other variables are extremely sensitive to τ_l and B_0 , surface pressure responds only weakly to variation in these parameters. A shock expansion calculation was carried out, and for $t \geq 0.35$ surface pressures are predicted quite accurately by a simple isentropic expansion. In this sense surface pressure is unaffected by the presence of radiation. Investigation of the ogival motion began at $t = 10^{-4}$ and required approximately two hours to IBM 7094 computation to reach $t = 0.4$.

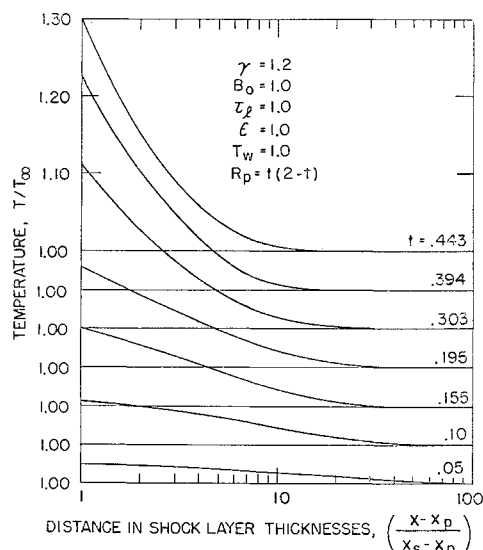


Fig. 7 Evolution of the flowfield induced upstream of the shock wave generated by a decelerating planar piston.

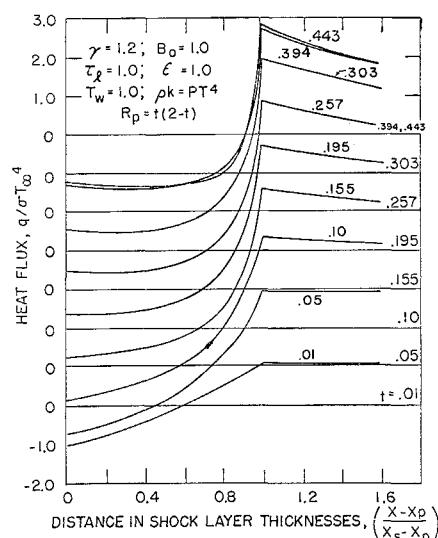


Fig. 8 Radiative field generated by a decelerating planar piston.

About ten seconds of IBM 7094 computation were required per time increment. When upstream absorption was neglected, new flowfields were generated ten times as rapidly.

Cylindrical Flowfields

Radiation coupled flows possess unique aspects which may be more prominent in axisymmetric than in planar fields. As opposed to chemically relaxing flows, the thermodynamic system composed only of the gas in question continually has energy flowing into or out of it at the piston surface. Therefore, the entropy layers usually present in chemical nonequilibrium need not exist in radiating flows. One may draw an analogy between the effects of surface temperature and emissivity upon these entropy layers when nonequilibrium radiation is present and that of wall blowing (or suction) and heating (or cooling) in viscous boundary layers. Perfectly reflecting walls in inviscid radiating flows correspond, for instance, to adiabatic walls in the viscous situation. No such analogy exists in inviscid, chemically reacting, nonradiating flows because no boundary data on nonequilibrium chemistry are allowed. These observations are best illustrated in cylindrical flowfields, wherein geometric effects may enhance relaxation.

The coupling between radiation and convection during the initiation of piston motion was more important in cylindrical than in planar geometries. It was confirmed that if the radiating flow were begun at a small enough time, the nonradiating, conical flowfield was correct. Extreme nonmonotonic behavior is observed in the evolution of surface pressure and the temperature of the gas at the wall, Fig. 9. Such be-

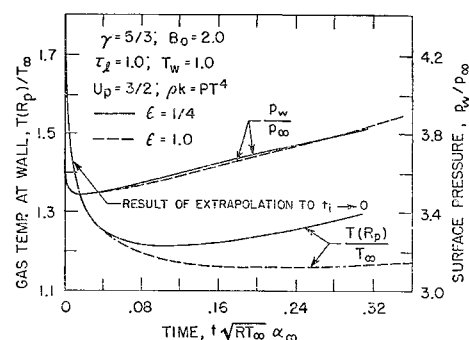


Fig. 9 The effect of emissivity upon temperature slip and pressure at the surface of a cylindrical piston in uniform motion.

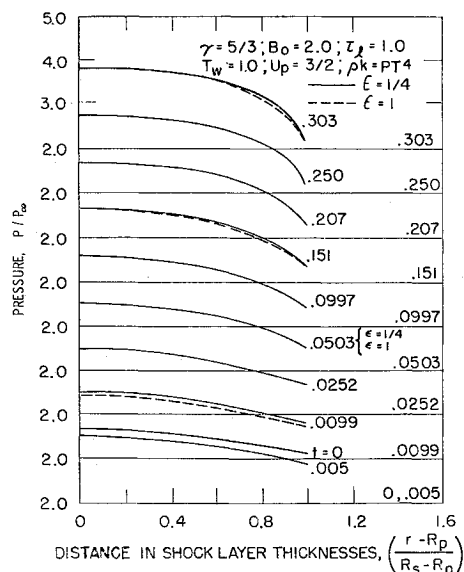


Fig. 10 Pressure field generated by a cylindrical piston in uniform motion.

havior was observed in wedge-like flows as well. The phenomenon is well documented in both ideal³³ and real³⁴ gas flows when vorticity accumulation occurs. The entropy bleeding effect of an absorbing wall is illustrated by the temperature distribution, and surface pressure is insensitive to emissivity. Since previous analyses of nonlinear problems in radiative gasdynamics have considered mainly black, cold walls, it is not surprising that nonmonotonic behavior of this type has not been reported. Of course, linear theory cannot be expected to predict the occurrence since it is due to complex nonlinear interactions.

Comparison of Figs. 10 and 11 with Figs. 5 and 6 dramatizes the smoothing effect of geometrical attenuation. The effect of emissivity on pressure is slight, but that upon temperature is pronounced. A small emissivity forces the majority of shock layer energy losses to occur through the shock rather than into the wall. Thus an entropy layer appears at the shock wave, Fig. 11, much more rapidly when emissivity is small. The net energy loss from the shock layer is nearly independent of emissivity. This is demonstrated by the insensitivity of shock shape (Fig. 12). If energy is lost to the wall ($\epsilon \approx 1$) it may not be recovered, but it is always available

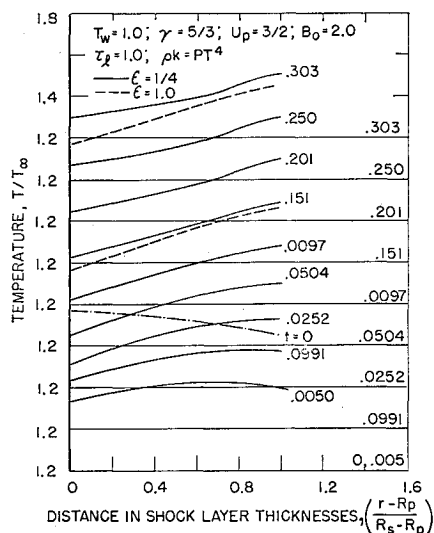


Fig. 11 Temperature field generated by a cylindrical piston in uniform motion.

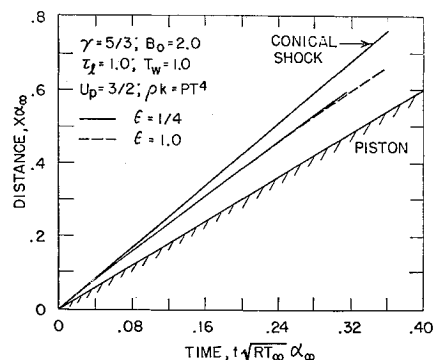


Fig. 12 Effect of emissivity upon shock wave generated by a cylindrical piston in uniform motion (e.g., 2° half-angle cone at 350 kft, 40,000 fps).

if it is absorbed by the gas upstream. This may have significant consequences upon subsequent motion.

The general insensitivity of most variables to variations in emissivity is predicted by the consistent boundary condition, Eq. (3.7). As emissivity decreases the second term is weighted more heavily than the first. In addition, the heat flux is constrained for small values of the optical variable, where the weight $\exp(-\tau_1 \eta^{3/2})$ is largest. Thus, the value of I_0 at the wall is insensitive to emissivity, and geometric effects may compensate for variations in surface properties. The inclusion of upstream absorption delayed the approach to radiative equilibrium sufficiently that it was not computationally feasible to pursue it. The multidimensional extension of the present analysis has been formulated. Further extensions in real gases are currently in progress.

Conclusions

The suitability of a characteristics approach to general problems in unsteady radiative gasdynamics has been demonstrated through the investigation of one-dimensional piston problems in ideal, radiating gases. The following general conclusions have been inferred as well. 1) Only Mark-type conditions are consistent with a P_1 differential approximation if upstream absorption of shock layer radiation is allowed. 2) The manner in which the radiative field is initiated numerically cannot affect entropy levels of the subsequent flow. 3) Nonlinear interaction of disturbances may be more important in radiative gasdynamics than in other nonequilibrium flows. It appears that at least one more order may be required in linearized analyses. 4) The differential approximation to radiative transfer is adequate for two-dimensional slender body flows. 5) Nonmonotonic behavior of surface properties may occur in radiating flows. 6) The pressure distributions along the surfaces of slender bodies are insensitive to large variations in parameters of the radiative field. The observable motion is insensitive to variations in emissivity. 7) Transverse absorption of shock layer radiation may be a dominant mechanism even in slender body flows.

It is hoped that the present approach will aid in the refinement of the design of slender re-entry vehicles.

References

- 1 Traugott, S. C., "A Differential Approximation for Radiative Transfer with Application to Normal Shock Structure," RR-34, Dec. 1962, Martin Co., Baltimore, Md.
- 2 Cheng, P., "Dynamics of a Radiating Gas with Application to Flow over a Wavy Wall," *AIAA Journal*, Vol. 4, No. 2, Feb. 1966, pp. 238-245.
- 3 Sauerwein, H., "Numerical Calculations of Arbitrary Multi-Dimensional and Unsteady Flows by the Method of Characteristics," AIAA Paper No. 66-412, Los Angeles, Calif., 1966.
- 4 Nemchinov, I. V., "Some Nonstationary Problems of Radia-

tive Heat Transfer," A & ES TT-4, Feb. 1964, Purdue University, Lafayette, Ind.

⁵ Chandrasekhar, S., *Radiative Transfer*, Dover, New York, 1960.

⁶ Simon, R., "The Conservation Equations of a Classical Plasma in the Presence of Radiation," *Journal of Quantitative Spectroscopy and Radiative Transfer*, Vol. 3, No. 1, Jan. 1963, pp. 1-14.

⁷ Bethe, H. A., "The Fireball in Air," *Journal of Quantitative Spectroscopy and Radiative Transfer*, Vol. 5, No. 1, Jan. 1965, pp. 9-12.

⁸ Finkleman, D., "Self-Consistent Solution of Nonlinear Problems in Unsteady Radiation-Gasdynamics," TR-147, Sept. 1967, Aerophysics Lab., Massachusetts Institute of Technology, Cambridge, Mass.

⁹ Jeffrey, A. and Taniuti, T., *Nonlinear Wave Propagation With Applications to Physics and Magnetohydrodynamics*, Academic Press, New York, 1964, Chaps. I and II.

¹⁰ Sachs, R. G., "Some Properties of Very Intense Shock Waves," *Physical Review*, Vol. 69, No. 9/10, May 1946, pp. 514-522.

¹¹ Courant, R. and Hilbert, D., *Methods of Mathematical Physics*, 1st ed., Vol. II, Interscience, New York, 1962, Chap. V, pp. 486 and 490.

¹² Marshak, R. E., "Effect of Radiation on Shock Wave Behavior," *The Physics of Fluids*, Vol. 1, No. 1, Jan.-Feb. 1958, pp. 24-29.

¹³ Sherman, M. P., "Moment Methods in Radiative Transfer Problems," *Journal of Quantitative Spectroscopy and Radiative Transfer*, Vol. 7, No. 1, Jan.-Feb. 1967, pp. 89-109.

¹⁴ Curtiss, C. F. and Hirschfelder, J. O., "Integration of Stiff Equations," *Proceedings of the National Academy of Sciences*, Vol. 38, No. 3, March 1952, pp. 235-243.

¹⁵ Heaslet, M. A. and Baldwin, B. S., "Predictions of the Structure of Radiation Resisted Shock Waves," *The Physics of Fluids*, Vol. 6, No. 6, June 1963, pp. 781-791.

¹⁶ Davison, B. and Sykes, J. B., *Neutron Transport Theory*, 1st ed., Clarendon Press, Oxford, 1958, pp. 129 ff.

¹⁷ Finkleman, D., "A Note on Boundary Conditions for Use with the Differential Approximation to Radiative Transfer," *International Journal of Heat and Mass Transfer*, Vol. 12, No. 5, May 1969, pp. 653-656.

¹⁸ Chou, P. E., Karpp, R. R., and Huang, S. L., "Numerical Calculation of Blast Waves by the Method of Characteristics," *AIAA Journal*, Vol. 5, No. 4, April 1967, 618-623.

¹⁹ Courant, R., Isaacson, W., and Rees, M., "On the Solution of Nonlinear Hyperbolic Differential Equations by Finite Dif-

ference," *Communications in Pure and Applied Mathematics*, Vol. 5, No. 3, Aug. 1952, pp. 243-255.

²⁰ Kourganoff, V., *Basic Methods in Transfer Problems*, Dover, New York, 1963, p. 90.

²¹ Vincenti, W. G. and Kruger, C. H., Jr., *Introduction to Physical Gasdynamics*, Wiley, New York, 1965, Chap. XII.

²² Abramowitz, M. and Stegun, I. A., *Handbook of Mathematical Functions with Formulas, Graphs, and Mathematical Tables*, AMS No. 55, June 1964, National Bureau of Standards, Washington, D.C., pp. 228-254.

²³ Xerikos, J. and Anderson, W. A., "A Critical Study of the Direct Blunt Body Integral Method," SM-42603, Dec. 1962, Douglas Aircraft Co., Santa Monica, Calif.

²⁴ Scala, S. M. and Gordon, P., "Solution of the Time-Dependent Navier-Stokes Equations for the Flow around a Circular Cylinder," AIAA Paper 67-221, New York, 1967.

²⁵ Taylor, G. I., "The Air Wave Surrounding an Expanding Sphere," *Proceedings of the Royal Society (London)*, Vol. A186, No. 1006, Sept. 1946, pp. 273-292.

²⁶ Hayes, W. D. and Probststein, R. F., *Hypersonic Flow Theory*, 1st ed., Academic Press, New York, 1959, pp. 35 ff.

²⁷ Wang, K. C., "Radiating and Absorbing Steady Flow over Symmetric Bodies," *Journal of Quantitative Spectroscopy and Radiative Transfer*, Vol. 8, No. 1, Jan. 1968, pp. 119-144.

²⁸ Kohsla, P. K., "Two Dimensional High Speed Flow of a Radiating Gas," *Journal of Quantitative Spectroscopy and Radiative Transfer*, Vol. 8, No. 1, Jan. 1968, pp. 145-160.

²⁹ Traugott, S. C., "Shock Structure in a Radiating, Heat Conducting, and Viscous Gas," *The Physics of Fluids*, Vol. 8, No. 5, May 1965, pp. 834-849.

³⁰ Kourganoff, V., "Sur L'Anisotropie du Rayonnement dans les Atmospheres Stellaires et les Er reurs qui en Resultant dans Les Approximations d'Eddington," *Astrophysika Norvegia*, Vol. 5, No. 1, Jan. 1957, pp. 1-18.

³¹ Zeldovich, Ya. B. and Raizer, Yu. P., *Physics of Shock Waves and High Temperature Hydrodynamic Phenomena*, Academic Press, New York, 1966, p. 147.

³² Main, R. P. and Bauer, E., "Equilibrium Opacities and Emissivities of Hydrocarbon-Air Mixtures at High Temperatures," *Journal of Quantitative Spectroscopy and Radiative Transfer*, Vol. 7, No. 4, July-Aug. 1967, pp. 527-537.

³³ Traugott, S. C., "Some Features of Supersonic and Hypersonic Flow about Blunted Cones," RM-64, March 1960, Martin Co., Baltimore, Md.

³⁴ Sussman, M. B., "Nonequilibrium Flow Fields Due to Spatial Piston Motions," TR-131, June 1966, Aerophysics Lab., Massachusetts Institute of Technology, Cambridge, Mass.